Occurrence of liquefaction in cyclic burial of a structure submitted to wave-actions and resting on the seabed

David Bonjean, Philippe Foray, Hervé Michallet

Occurrence of liquefaction in cyclic burial of a structure submitted to wave-actions and resting on the seabed

D. Bonjean & P. Foray
Laboratory 3S (Soils, Solides, Structures), Grenoble Technical University, France

H. Michallet
LEGI (Laboratoire des Ecoulements Géophysiques et Industriels), Grenoble Technical University, France

ABSTRACT: Coastal or offshore structures such as pipelines installed on the seabed are submitted to the hydrodynamic action of the waves either by a direct application of cyclic wave loads or through the cyclic movement of risers or flow lines transmitted by floating structures. In fine sandy or silty soils the cyclic loads can induce a liquefaction of the surrounding bed which can play an important part in the processes of erosion, trenching or self-burial of the pipes. A large 1 g physical model was built to study the fluid-soil-structure interaction with special emphasis on the conditions of occurrence of liquefaction around a pipe instrumented with pore pressure sensors. The experiments indicate a build up in pore pressure at the pipe-soil interface and a lateral visualisation showed a liquefaction of a soil band in the vicinity of the pipe. The penetration of the structure can be related to the phenomenon of liquefaction.

1 INTRODUCTION

An increasing attention has been given in recent years to the effect of wave-induced liquefaction on the stability of coastal or offshore structures. Field observations indicate that liquefaction can play an important part in erosion and stability problems for breakwaters or pipelines. Recent studies have focused on experimental and theoretical approaches towards the development of liquefaction of the entire seabed and the consequences on sinking or floatation of pipelines, see Sumer *et al* (1999), Sassa *et al* (2001), Cheng *et al* (2001), Teh *et al* (2003). Previous experimental works carried out by Lyons (1973), Lambrakos (1985), Brennoden *et al* (1986), Wagner *et al* (1986), Palmer *et al* (1988) were devoted to the specific pipe-soil interaction in order to elaborate design criteria for pipeline stability. A previous experimental program was conducted at the University of Grenoble by Branque *et al* (2002) to quantify the influence of the cyclic amplitude and the density of the sand on the penetration of the pipe and the evolution of the lateral resistance. A transitory liquefaction of the soil close to the pipe could be noted for some of the tests. Within the framework of the European program LIMAS ("Liquefaction around Marine Structures"), a new experimental research program was devoted to the fluid-soil-structure interaction, with an emphasis on pore pressure measurements at the pipe-soil interface and within the soil. The conditions of occurrence of liquefaction and their effect on the pipe stability were studied. The first experimental results are presented here. In most of these tests, the effects of the hydrodynamic forces were simulated by the application of cyclic loads or displacements on the pipe model. Nevertheless Damgaard & Palmer (2001) discussed the order of magnitude of the different processes leading to the instability of pipes and found that the hydrodynamic forces necessary to move laterally a pipe resting on the seabed induce sediment transport and liquefaction before a significant movement of the pipe occurs. Hence such experiments are more representative of the cyclic effects of a floating structure linked to flowlines or risers resting on the seabed.

2 INSTRUMENTAL SET-UP

2.1 *Testing tank*

The experimental set up constructed at the University of Grenoble by Branque (1998) is similar to the one used in the "Pipestab" research program performed by Brennoden *et al* (1986), Wolfram *et al* (1987). In the present research program, large modifications were made to the actual set up in order to allow a better control of the loading conditions and a lateral visualisation of the liquefaction process around the structure.

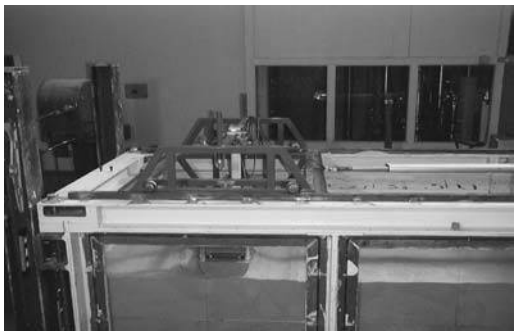

Figure 1. Experimental set up, with the electro-mechanic actuator set.

A large rigid tank of 2 m length, 1 m width and 1 m depth is filled with sand. One side of the tank is made of two glasses about 1 m × 1 m to allow direct visualisation of the strain in the sand. Figure 1 presents a general view of the experimental set up.

2.2 *Trolley and pipe model*

A trolley supporting a one-meter length pipeline section can roll on two horizontal rails along the length of the tank, parallel to the windows. The pipe itself is free to move vertically between two guides, and then to penetrate into the sand under its self-weight. Several (up to five) pore pressure transducers were installed on the external surface of the pipe in contact with the soil, and within the seabed, close to the pipe. In order to simplify the installation of the pore pressure transducers, a half-pipe with a diameter of 200 mm was used in the present experiments.

The connection between the section of the pipe and the glass is realized with a rubber joint. Thus it is possible to see a 2D cross section of the pipe-soil interaction, perpendicular to the axis of the pipe. Moreover, it was possible to record a video of the experiments showing the occurrence of liquefaction.

2.3 *Loading systems*

2.3.1 *Electro-mechanical actuator*

A mechanical actuator fixed on the tank can move the trolley horizontally. A load cell links the actuator to the trolley. The actuator is moved via a computer controlled electrical motor.

This set up allows a load-controlled regulation of the actuator. It is then possible to reproduce the cyclic wave-induced hydrodynamic forces acting on the pipeline.

2.3.2 *Motor set*

A different solicitation set up was also used in order to perform displacement controlled tests. A crankshaft-connecting rod system converts the circular motion into a horizontal sinusoidal movement. Despite such a device preventing load regulation of the movement, it does allow a much more accurate control of the pipe displacement. During the entire testing procedure, the horizontal amplitude of the displacement and the velocity of the pipe are strictly the same. Although such loading conditions do not represent exactly the hydrodynamic effects, they are interesting in order to understand the influence of the experimental parameters. This device is presented in Figure 2.

Figure 2. Loading system for displacement controlled tests.

2.4 *Transducers*

Druck PDCR 4030 pressure sensors were used. They allow the measurement of a relative pressure up to $7 \cdot 10^4$ Pa with a precision of 0.08%. This corresponds to an accuracy in the water height of about 0.5 mm.

2.5 *Saturation system*

A layer of gravel covered by a geotextile membrane is first installed at the bottom of the tank. Water can be circulated through this drainage system in order to saturate the sand bed by an uplift gradient. The gravel layer ensures a uniform distribution of the uplift gradient over the tank surface and a homogeneous saturation of the sand.

After filling the tank with water, the water table is kept at a level of about 10 cm above the sand surface to ensure it will remain saturated during the movement of the pipe.

2.6 *Sand characteristics*

The Fontainebleau sand used in the tests is a naturally-occurring, uniform, fine silica sand with sub-rounded grains of Tertiary, marine origin. It is remarkably pure, with 95 percent silica. It has been widely used as a standard "academic" sand in geotechnical laboratories in France.

Its main physical characteristics are: $D_{50} = 0.156\,mm$, $C_u = D_{60}/D_{10} = 1.47$, $D_{60} = 0.168$ mm, $D_{10} = 0.114\,mm$, $e_{max} = 1.06$, $e_{min} = 0.55$, $\gamma_{min} = 12.87\,kN/m^3$, $\gamma_{max} = 17.23\,kN/m^3$, $\gamma_s = 26.5\,kN/m^3$.

3 TESTING PROCEDURE

3.1 *Sand bed preparation*

3.1.1 *Dry method – loose sand*

When the tank is empty, we have the opportunity to set up the sand quite easily. We use a dry pluviation system. The sand is deposited with a low drop height. The lower the drop is, then the looser the sand arrangement will be. This method let us achieve quite loose sand, with a relative density I_D about 30%.

Once the whole sand required is in place, a very low uplift hydraulic gradient is applied at the bottom of the tank by the saturation system described earlier in this paper. This low gradient is more likely to let all air bubbles in the sand be pushed away by the water, instead of keeping them captive. This device helps achieve the best degree of saturation in the tank.

3.1.2 *Wet method – loose sand*

In order to allow more tests to be performed the entirety of the sand is not removed, dried and then set back in the tank between each tests. To reproduce the loose seabed, the dense one is just digged away, and then poured again by pluviation directly back into the water, without emptying the water.

Such a procedure produces again a loose sand mass, which density was found to be very similar to the one obtained by the dry method.

3.1.3 *Wet method – mid-dense sand*

Denser sand beds were prepared by vibrating initially loose sand with a vibratory rod. The vibration process was performed keeping the sand saturated. The relative density obtained by this procedure was about 60%.

3.2 *Load controlled tests*

The lateral forces to be applied to the pipe were calculated from hydrodynamic considerations and from the previous tests performed by Branque (1998). In these series of tests, the experimental parameters explored were the load amplitude (30 to 90 daN), the loading period (2 to 8 s) and the relative density of the sand (35% and 60%). During the tests, the cyclic horizontal displacements were recorded together with the pipe penetration and the pore pressures around the structure.

3.3 *Controlled displacement tests*

These tests cover basically the same experimental parameters. Periods from 1 s to 6 s were studied in the tests performed with the actuator, and a constant period of 15 s was applied for the tests with the eccentric sinusoidal movement. Amplitudes of the applied lateral displacements of the pipe varied from 10 to 160 mm. The corresponding evolution of the lateral force was recorded.

Table 1. Testing program.

Control type	Density (%)	Period (s)	Load (daN)	Amplitude (mm)
Load	35	4	50	–
Load	35	2	50	–
Load	60	4	50	–
Load	60	2	50	–
Load	60	4	30	–
Load	60	4	60	–
Load	60	4	90	–
Load	60	6	60	–
Displacement*	60	2	–	21
Load	60	8	60	–
Load	60	6	30	–
Displacement*	60	6	–	105
Displacement*	35	1	–	10
Load	35	6	60	–
Displacement**	35	15	–	80
Displacement**	35	15	–	120
Displacement**	35	15	–	160

* Performed with the actuator set.
** Performed with the motor set.

3.4 *Testing program*

Table 1 summarizes the tests performed.

4 PENETRATION OF THE PIPE UNDER CYCLIC LOADING

4.1 *Load controlled tests*

4.1.1 *Influence of the loading period*

Figure 3 represents the evolution of the vertical penetration of the pipe with the number of loading cycles for tests in dense sand with a force amplitude of 60 daN and loading periods of 4, 6 and 8 s. The highest penetration is observed for the shortest period and little difference is noted between the curves corresponding to 6 and 8 seconds. This result has to be compared to the evolution of the excess pore pressure measured along the pipe and represented on Figure 4: the highest values of the pore pressure are obtained for the shortest period. This suggests that the short period corresponds to loading conditions close to undrained conditions and that a partial drainage occurs for the periods of 6 and 8 s.

In fact, due to the regulation system used to control the actuator movements, the pipe moves faster for the smallest cycle period. If the period is short, the actuator has very little time to reach its regulation value, and then needs to move much faster. On the contrary, for a

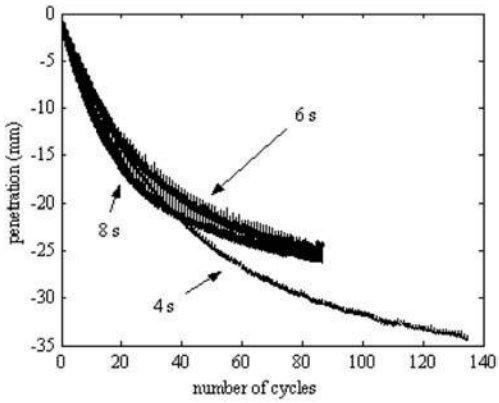

Figure 3. Influence of the loading period on the penetration of the pipe. Maximum applied load: 60 daN. Dense sand.

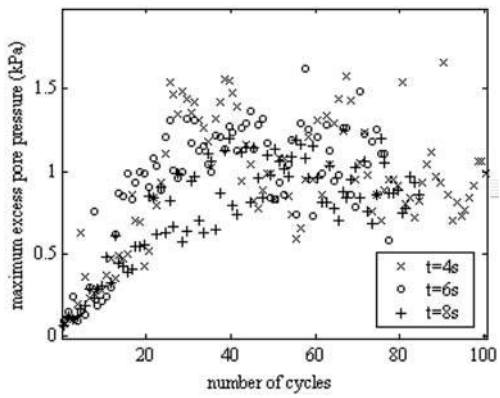

Figure 4. Influence of the loading period on the excess pore pressure at 60° under the pipe. Applied force amplitude: 60 daN. Dense sand.

long period the actuator don't need to move very fast to mobilize the prescribed resistance of the soil.

In this case, increase in peak pore pressure values is in close relation to the velocity of the actuator. For a given load, the smaller the period is, the faster the pipe moves, and the higher the maximum pore pressure generated is, because of a more "undrained" behaviour. For a more precise estimation of the drainage conditions it is necessary to compare the velocity of the pipe displacement to the sand permeability.

4.1.2 *Influence of the load amplitude*

The evolution of the penetration of the pipe as a function of time is represented in Figure 5 for a given period of 6 s and for three load amplitudes of 30, 60 and 90 daN. The value of 90 daN is close to the maximum horizontal resistance of the pipe in static conditions and it is logical to find a higher penetration of the pipe for a higher load amplitude.

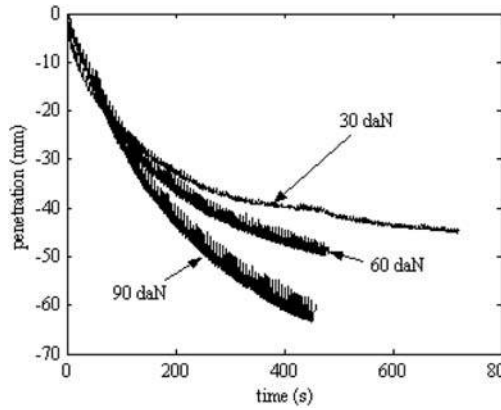

Figure 5. Influence of the load-amplitude on the penetration of the pipe, for a period T = 6 s. Dense sand.

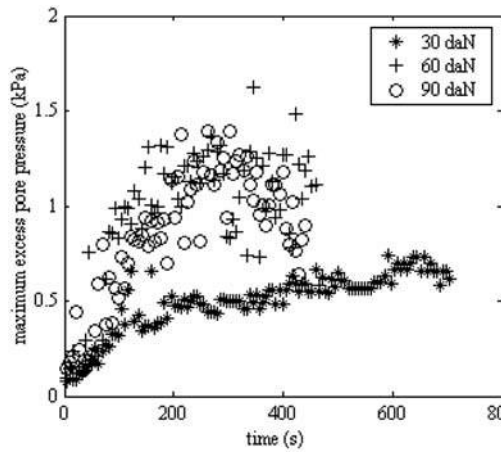

Figure 6. Influence of the load amplitude on the maximum excess pore pressure at 60° during each cycle. Period of cycles is 6 s. Dense sand.

The same corresponding trend is observed on the excess pore pressures at the pipe-soil interface: the lower pore pressure corresponds to the lowest load. All these tests suggest that the increase in pore pressure observed during each loading cycle is one of the key factors for the pipe penetration and consequently its loss of stability.

4.2 *Displacement controlled tests*

In this part, results obtained using the electromechanic actuator set are compared and discussed. Figures 7, 8 and 9 respectively present penetration, maximum pore pressure value, and maximum horizontal load developed.

The results seem to be in opposition with respect to the load controlled tests: the highest penetration is

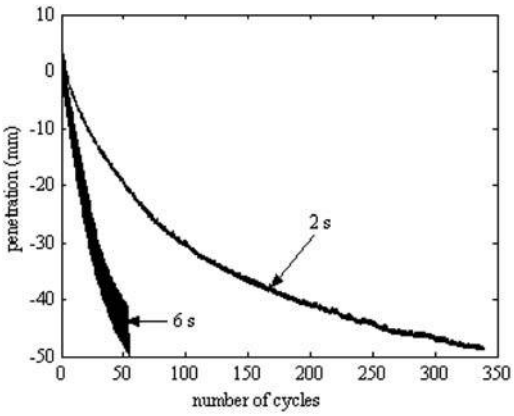

Figure 7. Influence of the loading period on the penetration of the pipe in a displacement controlled test. Displacement amplitude: 105 mm (Period T = 6 s), and 21 mm (Period T = 2 s) Dense sand.

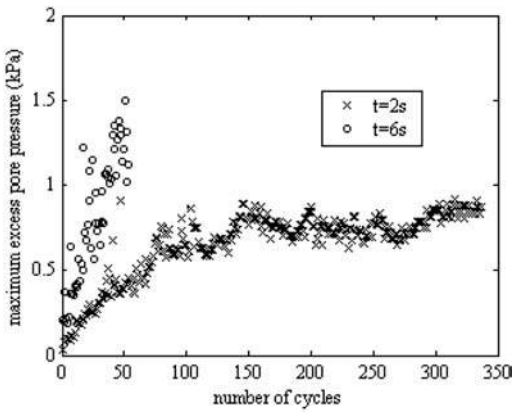

Figure 8. Influence of the loading period on the excess pore pressure at 60° under the pipe in a displacement controlled test. Displacement amplitude: 105 mm (Period T = 6 s), and 21 mm (Period T = 2 s) Dense sand.

observed for the largest period. At the same time higher excess pore pressures are also recorded for the larger period.

In fact, in these tests the higher period corresponds to a larger displacement amplitude, and consequently to a higher lateral resistance, as represented on Figure 9. These factors induce a larger penetration of the pipe.

This apparent contradiction can also be explained in terms of actuator velocity: in displacement controlled tests, for the given displacement amplitude and period, the velocity of the actuator is higher for the 6 s period. This confirms that the higher penetration and excess pore pressure are obtained when the loading conditions are close to undrained conditions.

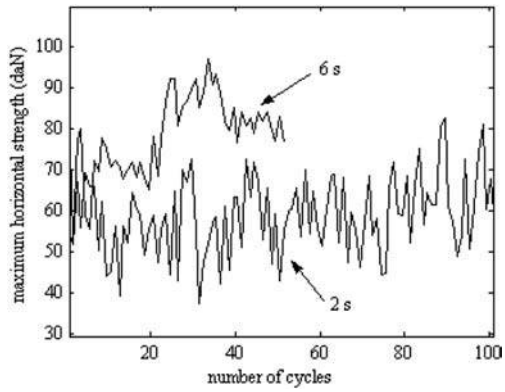

Figure 9. Maximum horizontal load measured in a displacement controlled test. Displacement amplitude: 105 mm (Period T = 6 s), and 21 mm (Period T = 2 s) Dense sand.

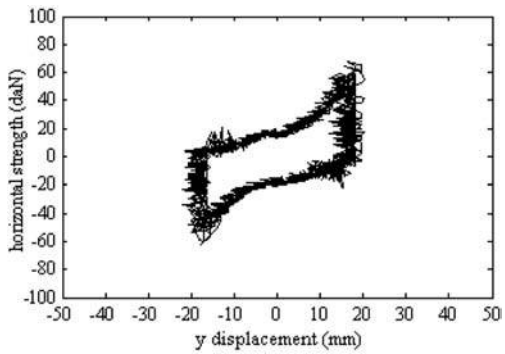

Figure 10. Controlled load test. Maximum horizontal load = 60 daN. Period T = 6 s.

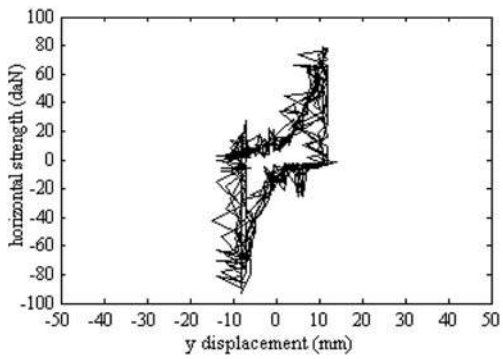

Figure 11. Controlled displacement test. Displacement amplitude = 21 mm, period T = 2 s.

4.3 *Cyclic load-displacement curves*

Typical cyclic load-displacement loops are presented in Figure 10 for a load-controlled test and in Figure 11 for a displacement controlled one. Despite some

dispersion in the experimental data, they show a very similar shape. For a similar load level, the inclination of the loops is governed by the displacement amplitude.

5 GENERATION OF PORE PRESSURE AT PIPE-SOIL INTERFACE AND LIQUEFACTION

5.1 *Set up description*

The pipe section was instrumented with five pore pressure transducers located all around the pipe. The respective positions of the transducers are shown in Figure 12. As it was not possible to install all the five transducers along the same cross section of the pipe, they were fixed on the pipe surface at different sections in the central part of the pipe. Therefore it is assumed that the distribution of the excess pore pressure is homogeneous along the length of the pipe. The pore pressure in the soil is transmitted to the transducer through a porous stone fixed at the connexion between pipe and transducer. This part was carefully saturated before each test.

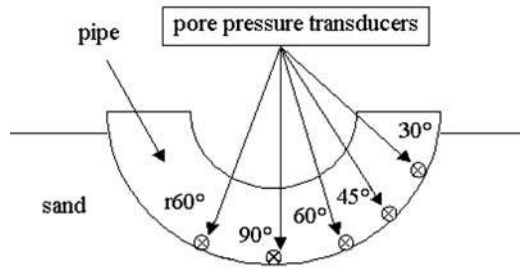

Figure 12. Distribution of the pore pressure sensors along the pipe-soil interface.

5.2 *Pore pressure recordings analysis*

5.2.1 *Excess pore pressure generation*

An example of the recordings obtained is presented in Figure 13. Every cycle, the pore pressure reaches a peak value greater than the vertical effective stress value at the same depth, assuming that: $\sigma'_v = \gamma' \times z$ where γ' is the submerged weight of the sand and z is the depth.

This level of excess pore pressure is sufficient to liquefy the sand.

According to the classical liquefaction theory, if $\sigma = \sigma' + u$, where σ is the total stress, σ' the effective stress and u the pore pressure, the excess pore pressure needed to liquefy the sand should be equal to the value of σ' in drained conditions. The classical earthquake liquefaction criteria compares the value of the excess pore pressure to the value of the initial effective overburden stress σ'_v. As an indication, Figure 13 shows excess pore pressure values compared with vertical effective stress at the same depth.

From the recordings presented in Figure 14, it is shown that the excess pore pressure reaches this level, and even a much higher value, more than twice. The high level of pore pressure generated indicates that the value of the effective vertical stress may not be the maximum mean effective stress found in the vicinity of the pipe. Due to the pipe pushing against the trench sides, horizontal stress in the sand may be greater than the vertical one. Using the simplified model developed by Branque *et al* (2002), the passive pressures mobilized along the pipe surface at the level of the pore

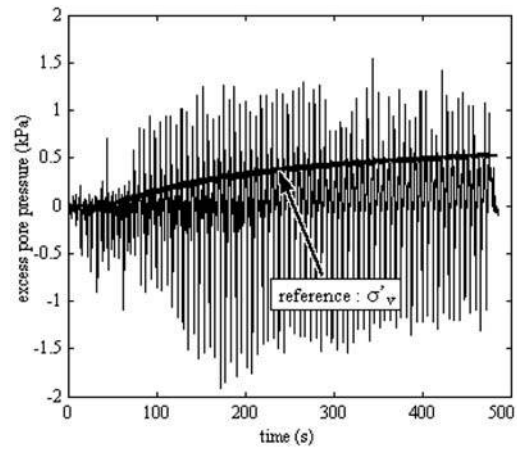

Figure 13. Excess pore pressure at 60° under the pipe and vertical principal stress at the same depth. Load controlled test. Maximum horizontal load is 60 daN, period is T = 6 s.

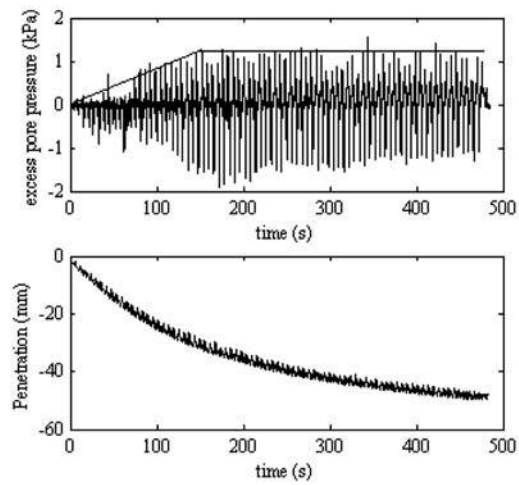

Figure 14. Load controlled test. Maximum horizontal load is 60 daN, period is T = 6 s. Dense sand.

pressure transducer (60°) could be calculated. In the case of the present experiments, they were found to be of the order of 6 kPa. The values of the peak pore pressures are intermediate between the passive pressure and σ'_v and should not exceed the mean effective stress under drained conditions.

5.2.2 *Maximum excess pore pressure value*

It is interesting to note that the maximum excess pore pressure value increases with the number of cycles at the beginning of the loading. For the same horizontal load applied by the actuator, the excess pore pressure generated is higher than the one developed during the previous cycle. For a given cycle, the behaviour of the seabed is dependent on the load history.

After a few cycles, the value of the maximum excess pore pressure tends to stabilize, although the pipe continues to sink.

This may confirm that a critical pore pressure value exists, corresponding to the initiation of liquefaction, which can not be exceeded. Furthermore this value is much greater than σ'_v, the vertical effective overburden stress. This indicates that the practical liquefaction criteria is conservative in this loading case due to the complicated stress path around the pipe. An intermediate stress between passive pressure and σ'_v would be more appropriate.

5.2.3 *Suction generation*

Each time the pipe changes direction and lifts off from trench side, depressions are measured. A kind of suction phenomenon is involved. The pipe tends to remain stuck to the side of the trench. Figure 13 and 14 shows such measurements every cycle.

At each cycle, the absolute value of the suction is greater than the excess pore pressure generated.

5.2.4 *Pore pressure distribution along the pipe*

The maximum amplitude of the pore pressure measured around the pipe is at 60° beneath the horizontal. The phenomena recorded at 45° are less important. However, the level reached by the excess pore pressure (about twice the effective vertical stress) seems great enough to liquefy the soil at this location.

On the other hand, the sensor set right under the pipe (90°) does not measure any excess pore pressure. The one at 30° measures only very weak variations of the pore pressure level. This is perhaps because it is very close to the surface, and the excess pore pressure has the opportunity to dissipate very quickly.

In fact the most significant pore pressure activity occurs in the range between 30° and 90°.

The transducer set on the other side of the pipe recorded pressure information very similar to its symmetrical counter part (60°). This confirms we have a symmetrical phenomenon, and that instrumenting one side on the pipe is sufficient in our case to monitor the whole burial process.

5.3 *Conclusions*

Excess pore pressure and then instant liquefaction occur each time the pipe is forcing into the trench bank. But no general liquefaction of the seabed occurs.

6 PORE PRESSURE RESPONSE IN SANDBED CLOSE TO THE PIPE

6.1 *Experience*

A series of tests have been performed, with two pore pressure transducers placed within the soil, as shown on Figure 15. The transducers were buried at a depth equal to half the maximum penetration allowed for the pipeline, and their minimum distance to the pipe was respectively 20 and 50 mm.

6.2 *Results analysis*

6.2.1 *Response*

Figure 16 represents the evolution of the excess pore pressure measured by the two transducers within the soil. The qualitative changes in pore pressure measured at the pipe-soil interface are reproduced with an attenuation according to the distance to the pipe.

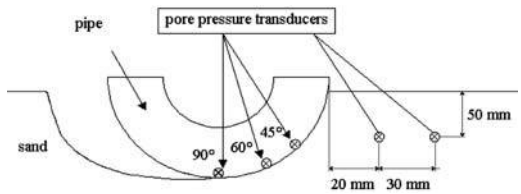

Figure 15. Location of the pore pressure sensors along the pipe and in the soil.

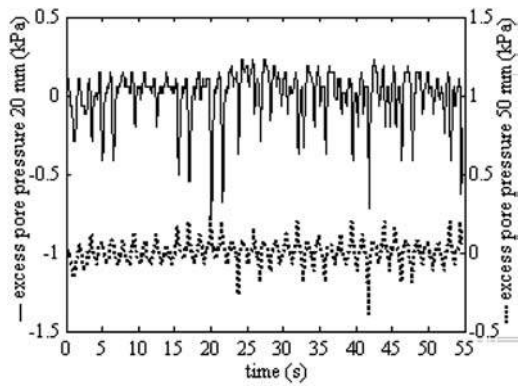

Figure 16. Recording of the pore pressure transducers placed within the soil. Controlled displacement test, performed with the electro-mechanical actuator set. Period T = 2 s.

The transducers show that, even within the soil, suction is felt when the pipe lifts off the trench side. During every cycle, absolute values of depression peaks remain greater than the value of the excess pore pressure generated. Thus, no build-up can occur, since the residual pore pressure level after any cycle is always the hydrostatic level.

6.2.2 *Mean level*

It appears that during the burial of the pipe, no build-up is measured. The average pore pressure in the soil is equal to the hydrostatic pressure at the same depth. But, each time the pipe comes into contact with the soil, a certain part of the sand reaches an inner excess pore pressure sufficient to liquefy instantaneously.

7 LIQUEFIED BEHAVIOUR

7.1 *Video transcription*

Some tests have been videoed, to allow accurate analysis of the seabed strains around the pipe during burial.

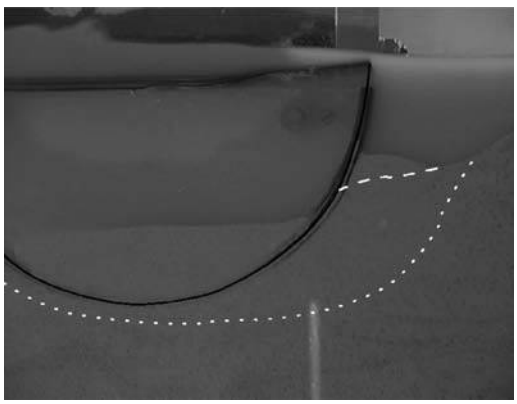

Figure 17a.

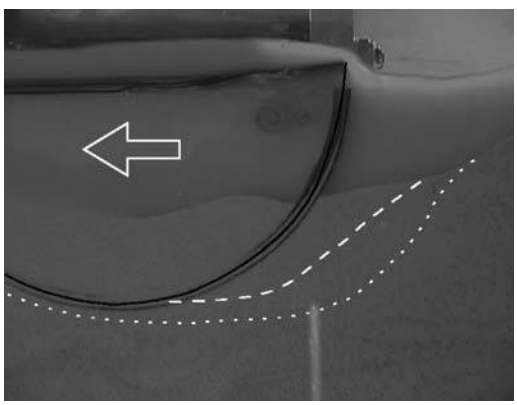

Figure 17b.

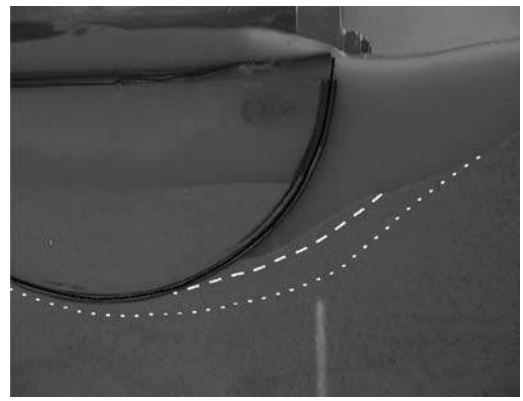

Figure 17c.

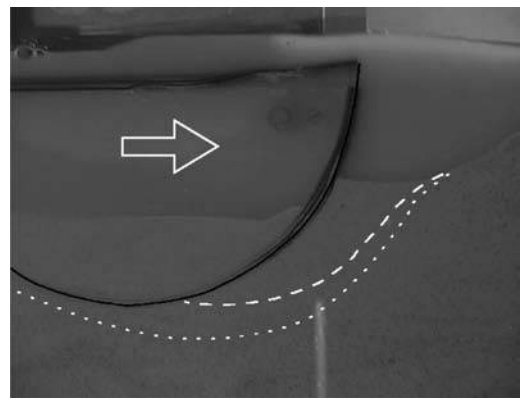

Figure 17d.

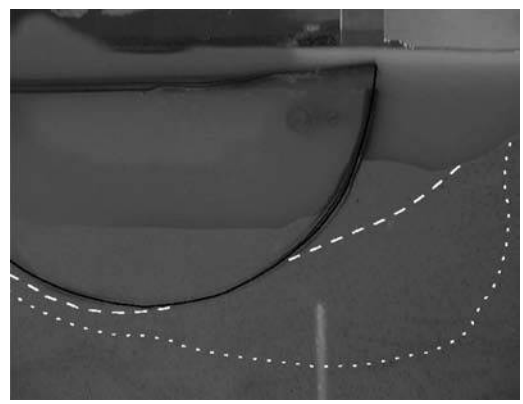

Figure 17e.

Figures 17a, b, c, d and e. Successive video frames over one period (2 s), controlled force test (maximum applied horizontal force: 50 daN). The grains mobility area is bounded by the dotted line (motions over the past 0.5 s). The liquefied area is bounded by the dashed line (flowing sand over the last 0.04 s).

An example of a series of video frame is given in Figures 17a, b, c, d and e.

It is obvious from these movies that a thin layer of sand close to the pipe behaves like a liquid. It flows away from the trench when the pipe moves towards the bank, and then flows under the pipe when it lifts off backwards.

It is also noticeable that a larger part of the bed is submitted to visible strains. A part of the soil seems to follow a plastic deformation along a circular failure line. This movement recalls plastic strains. This area is the one named "plastic behaviour" in Figure 18.

7.2 *Focus on drops of pore pressure measurements*

Figure 19 presents pore pressure recordings on the pipe surface at 60° below the horizontal of the pipe, and the corresponding lateral displacement of the trolley during the test. When the horizontal *y* position of the pipe increases, it moves in the direction towards where the pore pressure transducers are set. These are in contact with the trench side for the higher values of *y*.

It is noticeable that two different kinds of depression phenomena occur.

First, suction occurs when the pipe changes direction and starts lifting off from the trench side, just after the highest *y* displacement values (points marked 1 on Figure 19).

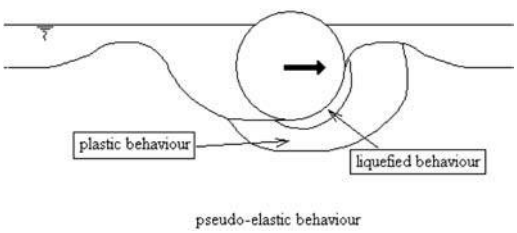

Figure 18. Scheme of different kinds of behaviour.

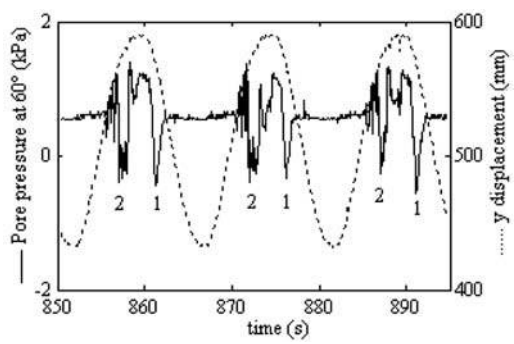

Figure 19. Controlled displacement test, performed with the motor set. Period T = 15 s. Displacement amplitude = 160 mm.

However, drops of pressure also appear when the pipe is pushing against the trench side, just before the maximum displacement, when *y* is still increasing. This drop of pressure is not a classical suction effect. It is not due to pulling like the first kind of depression. At this moment in the burial, the pore pressure transducer concerned is in contact with the sand, and the pipe continues to move in this direction. The pore pressure inside the bank begins to increase while the pipe is pushing in, and then drops. This might correspond to the moment when a critical pore pressure level is reached, and the sand liquefies. This liquefied layer is then pushed off the trench by the pipe, causing large displacements, important shears strains and dilatancy of this part of the sand. The increasing pore volume may cause the drop of pressure observed.

8 CONCLUSION

Direct visualisation of the self-burial process of a pipe submitted to hydrodynamic solicitations highlighted the influence of liquefaction in this phenomenon. An instantaneous liquefaction occurs at each cycle in a layer close to the pipe wall. This local and transitory liquefaction plays an important role in the burying of the pipe and its loss of stability. However no general liquefaction of the sandbed was induced by the cyclic movement of the pipe.

The set of parameters regulating the occurrence of liquefaction is complex, and further investigations are still needed. But main trends have already been pointed out. Especially, the velocity of solicitation with respect to the soil permeability, and thus the fact that the behaviour of the sand being more or less drained is one of the most important parameters.

If the conditions of pore pressure generation begin to be well understood, a good reference pore pressure level linked to the initiation of liquefaction remains to be determined. The classical liquefaction criteria using the effective vertical stress is not relevant in this case.

Despite no build up being involved here, it is noticeable that during the first few cycles, maximum pore pressure values gradually increases with the number of cycles, although the load applied remains constant.

Unexpected drops of pressure occur when the pipe is pushing against the sand. These seem to match with the flow of the liquefied sand.

ACKNOWLEDGEMENT

This study was partially funded by the European Commission Research Directorate, FP5, specific program "Energy, Environment and Sustainable Development", Contract No EVK3-CT-2000-00038, Liquefaction Around Marine Structures LIMAS.

REFERENCES

Branque, D. 1998. Etude de l'auto ensouillement des pipelines flexibles soumis à la houle et aux courants marins, *PhD Dissertation*, Institut National Polytechnique de Grenoble, 397 pages.

Branque, D., Foray, P. & Labanieh, S. 2002. Etude expérimentale de l'interaction entre les fonds marins et les pipelines flexibles soumis à la houle et aux courants, *Revue Française de Géotechnique.*

Branque, D., Foray, P. & Labanieh, S. 2002. Wave-induced interaction between soil and flexible pipelines resting on the seabed, in *Physical models in Geotechnics, Proc.Intern. Conf. of Physical Modelling in Geotechnics, St John, Newfoundland, Canada, July 2002*, Balkema Publishers, pp. 271–276.

Brennodden, H., Sveggen, O., Wagner, D.A. & Murff, J.D. 1986. Full scale pipe-soil interaction tests. In *Proceedings of 18th Offshore Technology Conference*, OTC 5338, Houston Texas.

Cheng, L., Sumer, B.M. & Fredsoe, J. 2001, Solutions of pore pressure build up due to progressive waves, *Int. J. Numerical and Analytical methods in Geomechanics,* 2001; 25, pp. 885–907.

Damgaard, J.S & Palmer, A.C. 2001. Pipeline stability on a mobile and liquefied seabed: a discussion of magnitudes and engineering implications. *In Proceedings of 20th Conference on Offshore Mechanics and Arctic Engineering*, OMAE'01, Rio de Janeiro, Brazil.

Lambrakos, K.F. 1985. Marine pipeline soil friction coefficient from in-situ testing. In *Ocean Engineering*, Vol.12, n° 2, pp. 131–150.

Lyons, C.G. 1973. Soil resistance to lateral sliding of marine pipelines. In *Proceedings of 5th Offshore Technology Conference*, OTC 1876, Houston, Texas.

Morris, D.V., Webb, R.E & Dunlap, W.A. 1988. Self-burial of laterally loaded offshore pipelines in weak sediments. In *Proceedings of 20th Offshore Technology Conference*, OTC 5855, Houston, Texas.

Palmer, A.C., Steenfelt J.S. & Jacobsen, V. 1988. Lateral resistance of marine pipelines on sand. In *Proceedings of 20th Offshore Technology Conference*, OTC 5853, Houston, Texas.

Sassa, S., Seikiguchi, H. & Miyamoto, J. 2001. Analysis of progressive liquefaction as a moving boundary problem, *Geotechnique* 51, N° 10, pp. 847–857.

Sumer, B.M., Fredsoe, J., Christensen, S. & Lind, M.T. 1999. Sinking/floatation of pipelines and other objects in liquefied soils under waves, *Coastal Engineering* 38, pp. 53–90.

Teh, T.C., Palmer, A.C. & Damgaard, J.S. 2002. Experimental study of marine pipelines on unstable and liquefied seabed, *Coastal Engineering, submitted July 2002.*

Wagner, D.A., Murff, J.D. & Brennodden, H. 1987. Pipe-soil interaction model. In *Proceedings of 19th Offshore Technology Conference*, OTC 5504, Houston, Texas.

Wolfram, W.R., Getz, J.R. & Verley, R.L.P. 1987. Pipestab Project: Improvement design basis for submarine pipeline stability. In *Proceedings of the 19th Offshore Technology Conference*, OTC 5501, Houston, Texas.